Armenian Journal of Physics, 2014, vol. 7, issue 4, pp. 201-212

FABRY-PEROT INTERFERENCE IN QUASI-PHASE-MATCHED SECOND HARMONIC GENERATION IN GREEN MICROCHIP LASER

M. Kerobyan[1,2,*], R. Kostanyan[1], S. Soghomonyan[2] and S. Essaian[2]
[1]*Institute for Physical Research, NAS RA, Ashtarak, Armenia*
[2]*Spectralus CJSC, Yerevan, Armenia*
[*]*e-mail: kerobyan.mk@gmail.com*

Received 20 September 2014

Abstract – We report on experimental and theoretical study of temperature tuning of single pass quasi-phase-matched second harmonic generation in a plane parallel PPMgOLN (periodically poled MgO doped LiNbO3) crystal in a green microchip laser. Periodic oscillations of second harmonic power upon variation of the temperature are observed. The oscillation period (4.8°C – 8.4°C) is several times smaller than the temperature acceptance bandwidth (18.4°C – 32.1°C), and the period strongly correlates with the crystal length. Formula for temperature dependence of second harmonic power is derived, which takes into account multiple reflections of fundamental and second harmonic waves in the nonlinear crystal. Comparison of experimental and theoretical data allows us to conclude that the origin of the oscillations is the multiple beam Fabry-Perot interference in the plane parallel nonlinear crystal.

Keywords: green microchip laser, second harmonic generation, Fabry-Perot interference

1. Introduction

Second harmonic generation (SHG) is widely used for nonlinear frequency conversion of laser radiation in various configurations, which involve single-pass setup, resonator-enhanced SHG, and intracavity SHG [1].

N. Bloembergen and P. S. Pershan have treated single-pass SHG in a plane parallel nonlinear crystal in [2] where they gave the solutions to Maxwell's equations in nonlinear dielectrics that satisfy the boundary conditions at a plane interface between linear and nonlinear medium.

Multiple beam interference effects in second harmonic generation in a plane-parallel nonlinear crystal were investigated in [3-8].

In [3] SHG in thin GaAs plate is investigated and rapid oscillations were found in the spectra, which are result of Fabry-Perot interference. SHG in wedged $LiNbO_3$ plate versus thickness of the plate was investigated in [4] and oscillations are found in the dependence of SH power versus thickness of the sample. This was the first observation of multiple beam interference in optical second harmonic generation.

When measuring optical coefficients, e.g. in Maker fringe technique, interference effects in SHG are very important. In [5, 6] authors took into account interference effects in SHG for more precise determination of optical coefficients. In [5], authors report on a method for measuring optical coefficients of thin semiconductor films, when Maker fringe technique is not

applicable. In [6] authors have presented a new formulation of Maker fringes in plane-parallel nonlinear crystals.

To achieve an accuracy of a few percent, effects of Fabry-Perot interference are taken into account in Maker fringe experiments [7]. In [8] authors report about development of theoretical expression for Maker fringe. A new formulation for Maker fringes has been given, using boundary conditions, anisotropy of the crystal, dispersion of the refractive index and multiple reflections of the fundamental and second harmonic waves in the nonlinear crystal.

In this paper we report on experimental and theoretical study of temperature tuning of single pass quasi-phase matched SHG in plane parallel nonlinear crystal.

The motivation for conducting this study is development of compact microchip laser with intracavity frequency doubling [9]. Microchip lasers are of interest and recent achievements are presented in [10-13].During temperature tuning test of the microchip lasers it was observed that some lasers show unexpected periodic oscillations of output power upon variation of the temperature. These oscillations hamper the temperature tuning of the microchip lasers, thus we need to understand the origin of oscillation to prevent it. For this reason we have investigated temperature dependence of second harmonic power for a nominally single-pass SHG in the nonlinear crystal similar to the crystal used in the microchip laser.

The outline of the paper is as follows. In Section 2, experimental work is described, including measurements of temperature dependence of output intensity of the microchip laser and temperature dependence of single pass SHG intensity in plane parallel nonlinear crystal. In the section 3, theoretical calculations are presented and compared to the experimental data. Section 4 and 5 are conclusion and acknowledgments respectively. Finally, paper ends with the appendix, where detailed solution of the wave equation for the second harmonic field is presented, which includes Fabry-Perot interference effects.

2. Experimental

2.1. Microchip laser output power versus temperature

Microchip lasers with intracavity frequency doubling are DPSS (diode pump solid state) lasers. Cavity of such a laser consist of two planar components: Gain crystal (Nd^{3+}:YVO_4), and nonlinear crystal (periodically polled MgO:$LiNbO_3$ – PPMgOLN), which are joined by optical contacting technique. The input face of the gain crystal is coated for high transmission (HT) at pump wavelength (808 nm) and high reflection (HR) at fundamental (1064 nm) and second harmonic (532 nm) wavelengths. The output face of the nonlinear crystal is coated for HT at 532

nm and HR at 1064 nm. To convert 1064 nm to 532 nm, quasi-phase matched second harmonic generation is used. To have maximum efficiency, temperature of the laser cavity should be fixed at optimal quasi-phase matching temperature.

Experimental setup, which is used to measure the temperature dependence of output power of the microchip laser, is depicted in Fig.1. Temperatures of the pump laser diode (LD) and microchip (MC) are controlled with the TEC1 and TEC2. Microchip laser is pumped with 808 nm wavelength and output power at 532 nm was registered. To reduce wavelength fluctuations, temperature of the LD is fixed during the experiment with the precision of $0.1°C$. Temperature of the MC is changed in the range of $25-70°C$.

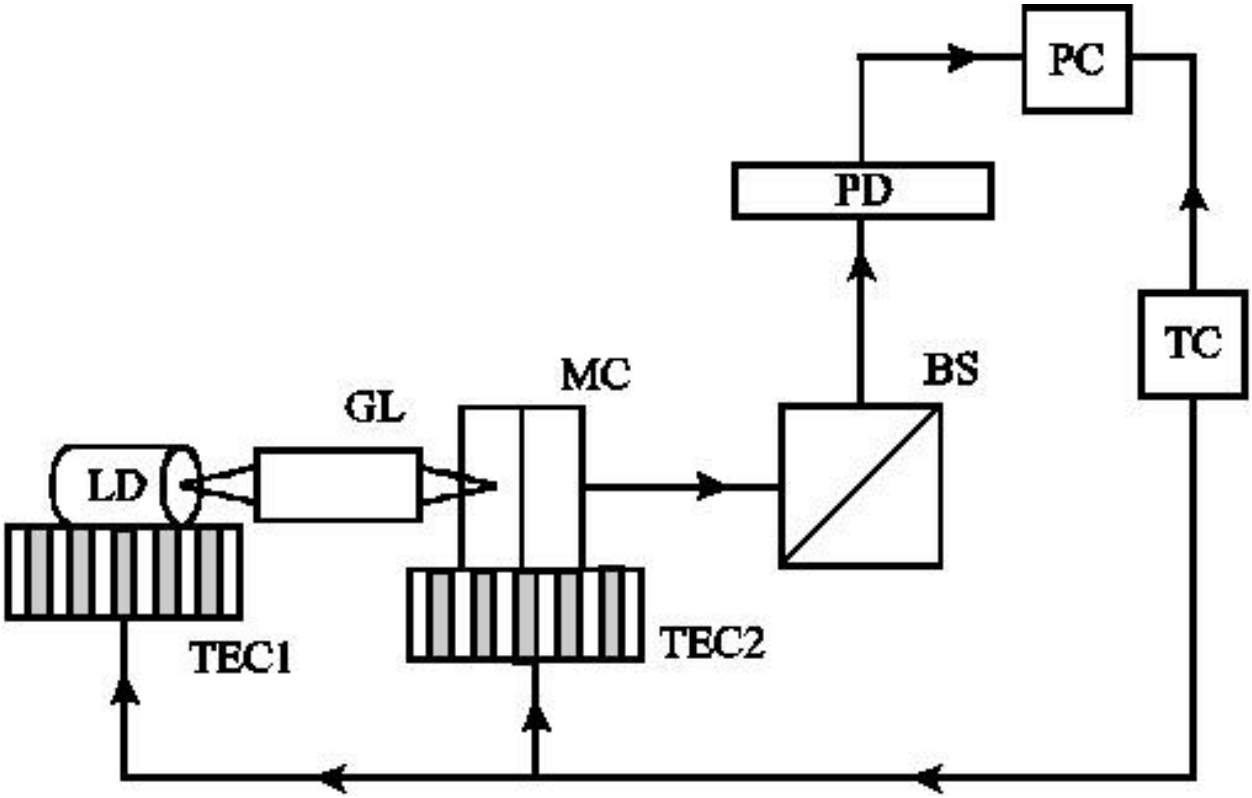

Fig.1. Schematic drawing of the experiment of measuring temperature dependence of microchip output power. LD – laser diode, GL – GRIN lens, MC – microchip, TEC1 – Thermo-electro cooler for the LD, TEC2 – Thermo-electro cooler for the MC, BS – beam splitter, PD – Photodetector, TC – Temperature controller, PC – Computer.

Results of the experiments for two different microchip lasers are shown in Fig.2. The first curve is relatively flat (Fig.2a), while the second one has clearly pronounced periodic oscillations (Fig.2b). The decline of the output power over the range of $25-55°C$ is due to temperature acceptance bandwidth δT in quasi-phase matched second harmonic generation, which is $18.4°C$ in case of plane wave approximation and 1.5 mm length of nonlinear crystal.

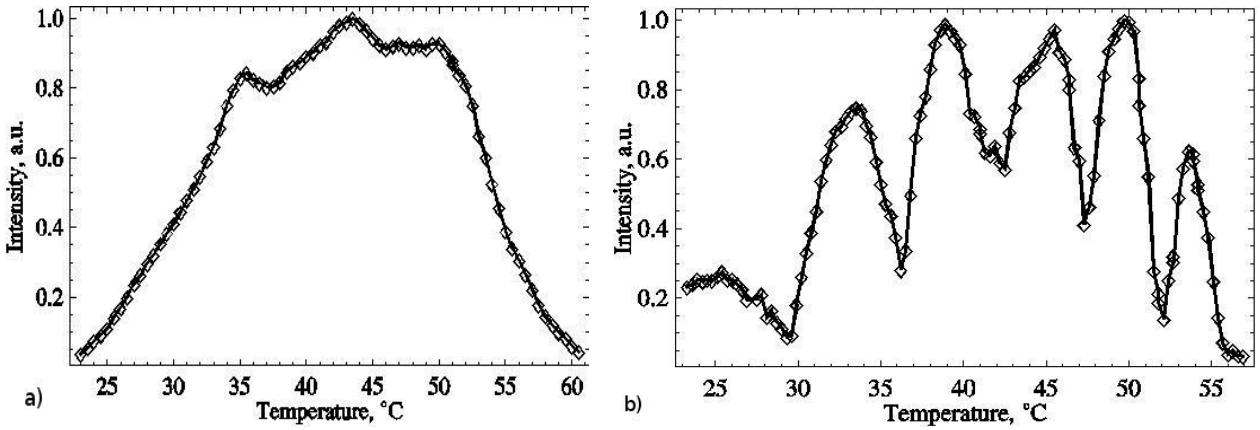

Fig.2. Microchip output power versus temperature for two different MC lasers. a) Relatively flat curve, b) Clearly pronounced periodic oscillations.

Measuring reflection from the contacted interface between gain crystal and nonlinear crystal for these two microchip lasers, it is found that reflection from the interface for second microchip is higher than for the first one [14].

These results were partially reported in [15], where it was assumed that these oscillations come from multiple reflections of fundamental and second harmonic beams in nonlinear crystal. To test this assumption single pass SHG experiments in the nonlinear crystal identical to those used in the microchip laser are conducted, and detailed calculations of second harmonic intensity in a nonlinear crystal is presented, which takes into account multiple beam interference of fundamental and second harmonic waves.

2.2. Single pass SHG in plane parallel nonlinear crystal

Experimental setup for measuring temperature dependence of SH intensity in single pass SHG is shown in Fig.3. 1064nm CW, single longitudinal mode laser is used as a pump. Pump beam is focused in the nonlinear crystal (PPMgOLN), and output power is registered by a photodiode. Polarization of the pump and SH waves are parallel to the c-axis of the nonlinear crystal. Temperature of the PPMgOLN is controlled by a thermo-electro cooler.

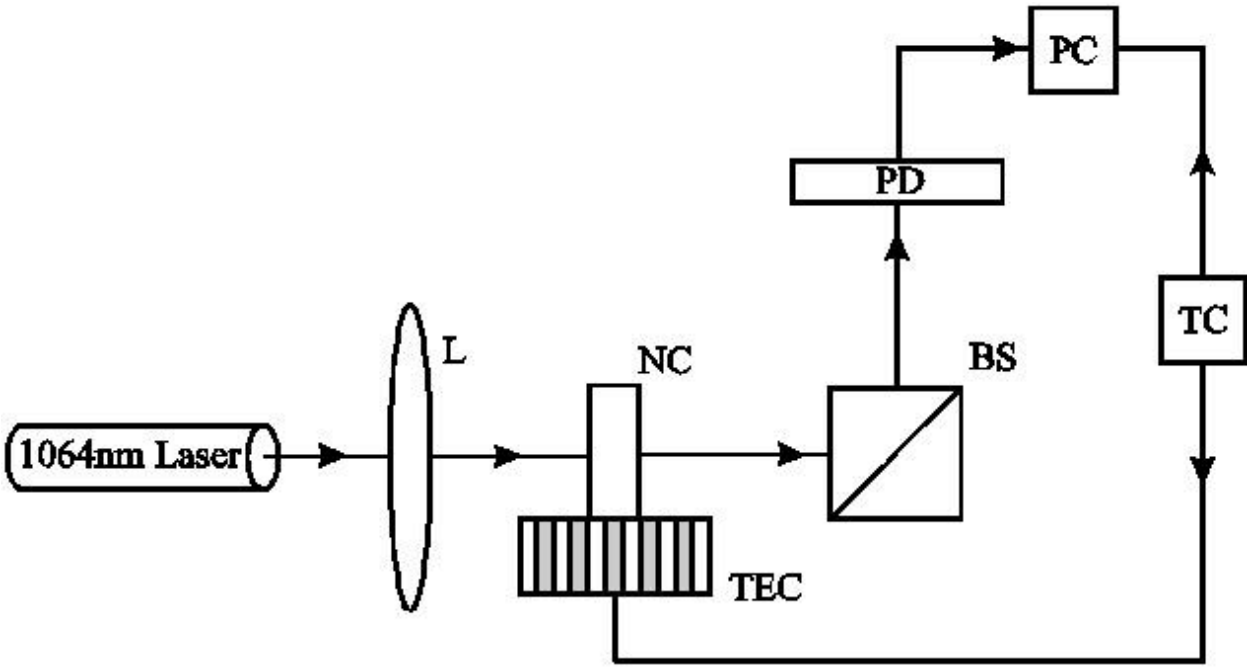

Fig.3. Schematic drawing of the experiment of measuring temperature dependence of single pass SHG. L – lens, NC – nonlinear crystal, TEC – Thermo-electro cooler, BS – beam splitter, PD – Photodetector, TC – Temperature controller, PC – Computer.

The input face of the PPMgOLN is polished, while the output face is coated for HT at 532 nm and HR at 1064 nm. Experiments are done on three crystals with different thickness. In Fig.4 results of the experiments is plotted with markers. It can be seen that observed oscillation periods τ_O correlate with the length of the PPMgOLN. Oscillations periods are equal to $\tau_O = (5.1 \pm 0.5)°\text{C}$ for l = 1.5 mm, $\tau_O = (6.3 \pm 0.5)°\text{C}$ for l = 1.17 mm and $\tau_O = (8.5 \pm 0.5)°\text{C}$ for l = 0.86 mm. This allows us to suppose that oscillations are result of interference between multiply reflected waves in NC.

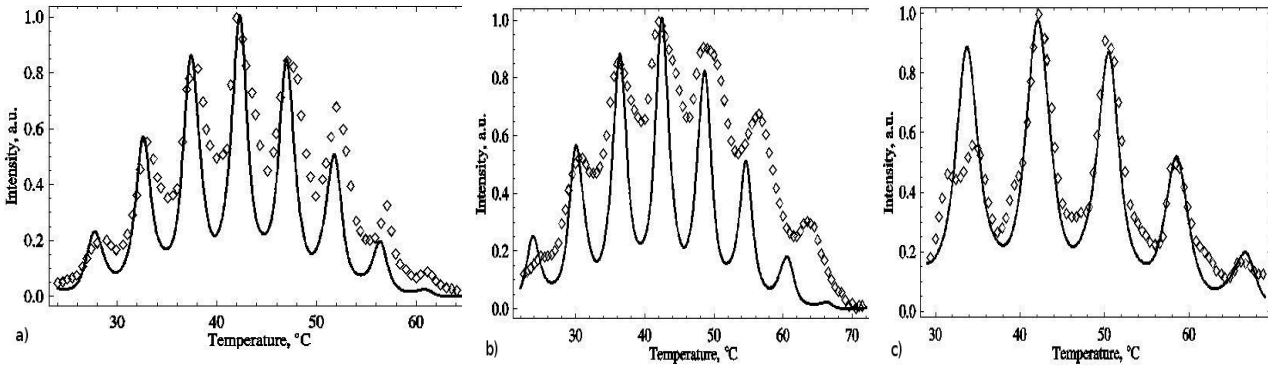

Fig.4. Observed (markers) and calculated (solid line) intensity versus temperature for single pass SHG. a) $l = 1.5mm, \tau_O = (5.1 \pm 0.5)°C, \tau_C = 4.8°C$, b) $l = 1.17mm, \tau_O = (6.3 \pm 0.5)°C, \tau_C = 6.1°C$, c) $l = 0.86mm, \tau_O = (8.5 \pm 0.5)°C, \tau_C = 8.4°C$

To test this hypothesis, in the experiment with the l = 1.5 mm length crystal, pump beam incidence angle is changed. Instead of perpendicular incidence, now incidence angle is equal to 5^{o}. This tilt angle provides poor overlap between multiple reflections, so they are not able to interfere. In the second experiment, the input face of the PPMgOLN is coated for HT at 1064 nm and HR at 532 nm. This coating eliminates multiple reflections. Results of these experiments are shown in Fig.5 (markers).

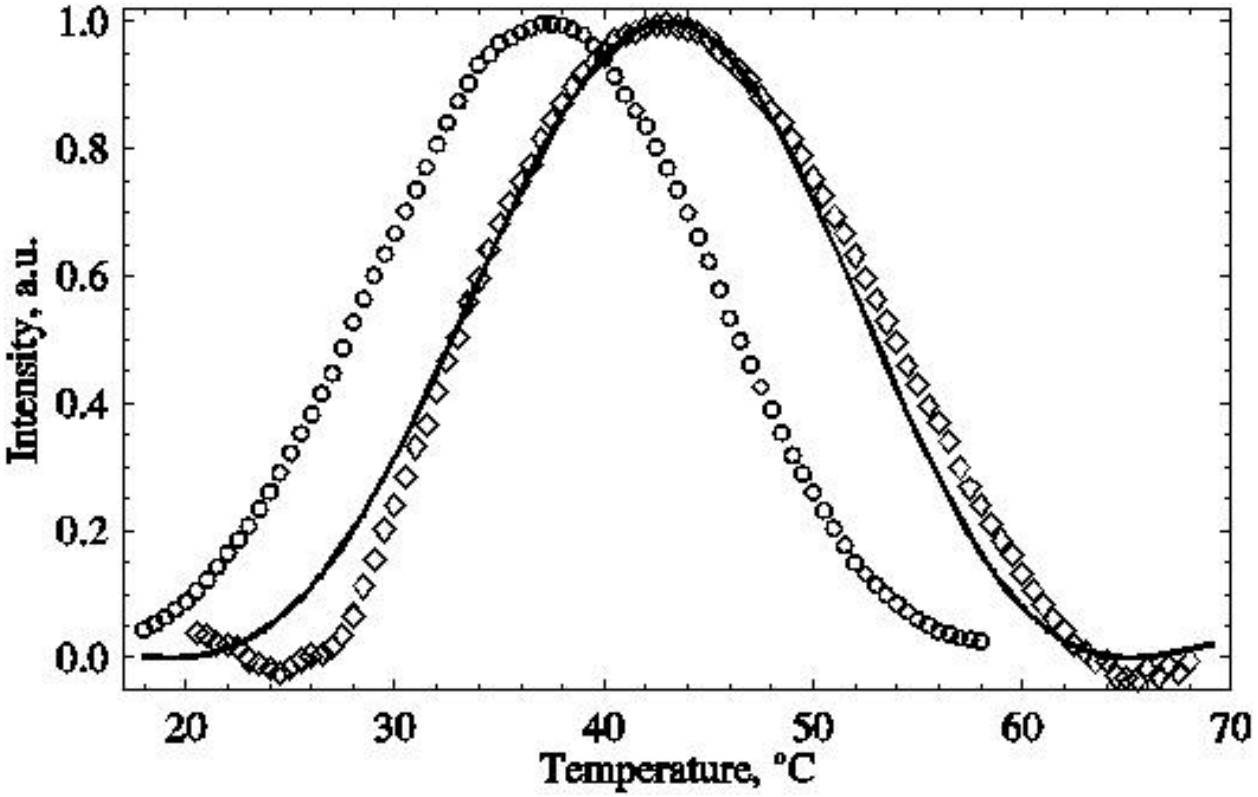

Fig.5. SH intensity versus temperature for $l = 1.5$mm $LiNbO_3$. Oblique incidence (○ – observed) and double side coating (◊ – observed, solid line – calculated).

One can see that if multiple reflections are absent or do not interfere, temperature curve of the SH intensity is smooth (without oscillations). In case of oblique incidence, the curve is shifted to the smaller temperatures. This is due to change of effective domain period $\Lambda^{*} = \Lambda / \cos\theta$, where Λ is the domain period and θ is the angle between beam and normal of the domain walls inside the nonlinear crystal. Optimal phase matching temperature (peak of the curve) can be found solving $\Delta k(T) = 2k_1(T) - k_2(T) - \cos(\theta)/\Lambda(T) = 0$ (wave vector mismatch is equal to zero, see Appendix 1 for details) equation for T in case of $\theta = 5° / n_1 = 2.27°$, where n_1 is the refractive index of the nonlinear crystal at pump wavelength. Solution of the equation is $T_0 = 37.9°\text{C}$, which is observed in the experiment.

3. Theory

To understand the reason of oscillations, let us suppose a pump wave is shone normally onto the nonlinear crystal's surface. Pump wave polarization is parallel to the c-axis of the nonlinear crystal. We need to solve wave equation for second harmonic field [16]

$$-\frac{d^2}{dz^2}E_2(z)-\frac{\omega_2^2}{c^2}\varepsilon_2 E_2(z)=\frac{4\pi\omega_2^2}{c^2}P_{NL}(z), \qquad (1)$$

where $E_2(z)$ is the amplitude of SH wave inside the NC, ε_2 is the dielectric susceptibility of crystal, ω_2 is the frequency of the second harmonic wave, c is the speed of light. $P_{NL}=4d_{eff}E_1^2$ is the nonlinear polarization, where d_{eff} is an effective nonlinear susceptibility.

As it was mentioned above, polarizations of the pump and SH waves are parallel to the c-axis of the crystal, so both waves have extraordinary polarization with respect to the crystal (type-0 SHG).

Detailed calculations are not presented in this paragraph, one can find them in the Appendix 1, where detailed solution of the wave equation for the second harmonic wave is presented. Here three major approximations will be discussed, which are used during solution of the wave equation.

First, monochromatic plane wave approximation. In the experiments Nd^{3+}:YVO_4 CW single longitudinal mode laser is used as a pump, which can be considered monochromatic. Positive lens is used to focus pump wave in the nonlinear crystal. Pump beam divergence full angle is $\Theta\approx 4.2\,\text{mrad}$ and output beam diameter is $\Omega_0=0.34\,\text{mm}$, focusing length of the lens is $f=25\,\text{mm}$ and it is located $d=540\,\text{mm}$ far from the laser source. Beam diameter at the focus can be estimated as $2\omega_0\approx 4f\lambda n/\pi(\Omega_0+d\Theta)\approx 28.6\,\mu\text{m}$. Rayleigh length is equal to $Z_R=\pi\omega_0^2 n_1/\lambda\approx 1328\,\mu\text{m}$. It is known, that at the focusing point wave front of the Gaussian beam is a plane. As long as Rayleigh length is comparable with the length of the crystal, wave in the crystal can be considered a plane wave.

Second, undepleted pump approximation. In the experiments, pump power is 100 mW. With this pump power maximal observed SH power was about 100 μW, which is negligibly small compared to the pump. Thus, pump wave can be considered to be undepleted during the propagation trough the nonlinear crystal.

It is usually allowed to neglect second order derivative of the amplitude $A_2(z)$. It is the third approximation, called slowly-varying amplitude approximation. It requires fractional

change of the SH wave amplitude on the distance of order of optical wavelength be much smaller than unity $\left|d^2A_2^{\pm}/dz^2\right| \ll \left|k_2(dA_2^{\pm}/dz)\right|$.

Solution of the wave equation (1) will give us the following expression for the amplitude of the SH wave (Eq.(A12))

$$A_2^{+}(l) = Cl\,\mathrm{sinc}\left(\frac{\Delta kl}{2}\right)\frac{\left(A_1^{+}\right)^2 e^{i\frac{\Delta kl}{2}} + r_1^{'}\left(A_1^{-}\right)^2 e^{-i\frac{\Delta kl}{2}}}{ik_2(1-\mathrm{r}_1^{'}\mathrm{r}_2^{'}\mathrm{e}^{2ik_2l})}. \tag{2}$$

Output intensity is proportional to the square of the absolute value of it. It is expressed in a compact form

$$I_2 \propto \left|E_0\right|^4 \mathrm{sinc}^2\left(\frac{\Delta kl}{2}\right)\left(FP_1\right)^2 FP_2\ , \tag{3}$$

where

$$\begin{aligned} FP_1 &= \frac{1}{1+F_1\sin^2\left(k_1l\right)} \\ FP_2 &= \frac{1}{1+F_2\sin^2\left(k_2l\right)} \end{aligned} \tag{4}$$

are the Airy functions describing multiple beam interference, with the following finesse coefficients

$$F_1 = \frac{4r_1r_2}{\left(1+r_1r_2\right)^2}, F_2 = \frac{4r_1^{'}r_2^{'}}{\left(1+r_1^{'}r_2^{'}\right)^2}\ . \tag{5}$$

It can be seen from the Eq.2 that SH intensity is modulated with two oscillating functions. Quasi-phase matching condition depends on the temperature through the wave vector mismatch $\Delta k = 2k_1(\mathrm{T}) - \mathrm{k}_2(T) - 1/\Lambda(T)$, where wave vectors of the fundamental and SH waves $k_1(T) = 2\pi n_1(\mathrm{T})/\lambda_1$ and $k_2(T) = 2\pi n_2(\mathrm{T})/\lambda_2$ depends on the temperature through the refractive index (thermo-optic effect $dn/dT \neq 0$), and domain period $\Lambda(T)$ depends on the temperature because of the thermal expansion. Besides, temperature variation due to thermal expansion and thermo-optic effect leads to the variation of the optical length of the crystal, which affect Airy functions.

In Fig.4 calculated temperature dependence of SH intensity for $l = 1.5$ mm, $l = 1.17$ mm and $l = 0.86$ mm crystals are presented with solid lines. It can be seen that observed and calculated oscillations periods are in an agreement. There are difference between calculated and observed oscillations amplitudes. For all three samples, observed amplitudes ale lower that calculated ones. The reason can be in the plane wave approximation and perpendicular incidence. In the experiment, pump wave is not exactly plane wave and not exactly

perpendicular to the nonlinear crystal surface. These factors lowers Fabry-Perot etalon finesse and leads to the minimization of the oscillations amplitude.

In Fig.5 calculated temperature dependence of SH intensity for $l = 1.5\,\text{mm}$ length crystal with double side coating is presented with solid line. As it is observed in the experiment, curve is Sinc (Sine cardinal) function, without any Fabry-Perot oscillations.

4. Summary

In summary, it is shown that oscillations in the temperature dependence of single pass SHG are result of the multiple beam interference in the nonlinear crystal. Formula for temperature dependence of single pass SHG intensity is derived. Formula includes multiple beam interference for fundamental and for second harmonic waves. Period of oscillations is inversely proportional to the length of the crystal. Theoretically calculated oscillations periods for PPLN with different thickness are in an agreement with the observed values. It is supposed, that origin of oscillations in the temperature dependence of the microchip output power is in the multiple beam interference in the resonator of the microchip laser, and studies are in progress.

Appendix 1

In this appendix, detailed solution of the wave equation for second harmonic wave in nonlinear crystal is presented.

Suppose amplitude of the incidence wave is equal to E_0 and it is a plane wave. Due to multiple reflections from the boundaries in the NC there will be two waves, propagating in the opposite directions

$$E_1^+(z) = it_1E_0e^{i(k_1z-\omega_1t)}\sum_{j=0}^{\infty} r_1r_2e^{2ik_1l} = \frac{it_1E_0}{1-r_1r_2e^{2ik_1l}}e^{i(k_1z-\omega_1t)}, \qquad \text{(A1)}$$

$$E_1^-(z) = it_1r_2E_0e^{i(-k_1z-\omega_1t)}\sum_{j=0}^{\infty} r_1r_2e^{2ik_1l} = \frac{it_1r_2E_0}{1-r_1r_2e^{2ik_1l}}e^{i(-k_1z-\omega_1t)}. \qquad \text{(A2)}$$

These are amplitudes of the waves in the NC, '+'and '– ' indicate forward (right) and backward (left) propagating waves, r_1, r_2 and t_1, t_2 are amplitude reflectance and transmittance coefficients of the first and second mirrors respectively. k_1 and ω_1 are the wave vector and frequency of the incidence wave in the NC, l is the length of the NC, z is a coordinate in the propagation direction and t is the time.

In the every point inside NC fundamental wave amplitude is a sum of $E_1^+(z) = \mathrm{A}_1^+ e^{i(\mathrm{k}_1z-\omega_1t)}$ and $E_1^-(z) = \mathrm{A}_1^- e^{i(-\mathrm{k}_1z-\omega_1t)}$, where $\mathrm{A}_1^+ = it_1E_0 / \left(1-r_1r_2e^{2ik_1l}\right)$ and $\mathrm{A}_1^- = it_1r_2E_0 / \left(1-r_1r_2e^{2ik_1l}\right)$. So, nonlinear polarization in the wave equation (1) will be equal to

$P_{NL} = 4d_{eff}\left(\left(A_1^+\right)^2 e^{2ik_1 z} + \left(A_1^-\right)^2 e^{-2ik_1 z} + 2A_1^+ A_1^-\right)$. Here $e^{-2i\omega_1 t}$ and $e^{-i\omega_2 t}$ terms are omitted, because $\omega_2 = 2\omega_1$ and they shrink each other in the wave equation. Because pump wave is a sum of opposite propagating waves, it is reasonable to look for a solution in the form of sum of opposite propagating waves

$$E_2(z) = \mathrm{A}_2^+(z)e^{ik_2 z} + \mathrm{A}_2^-(z)e^{-ik_2 z} \ . \tag{A3}$$

Substituting Eq.A5 and Eq.A3 into the Eq.A4 will give

$$\begin{aligned} &-\left(\frac{d^2A_2^+}{dz^2} + 2ik_2\frac{dA_2^+}{dz} - k_2^2\right)e^{ik_2 z} - \left(\frac{d^2A_2^-}{dz^2} - 2ik_2\frac{dA_2^-}{dz} - k_2^2\right)e^{-ik_2 z} - \frac{\omega_2^2\varepsilon_2}{c^2}\left(A_2^+e^{ik_2 z} + A_2^-e^{-ik_2 z}\right) = \\ &= \frac{16\pi d_{eff}\omega_2^2}{c^2}\left(\left(A_1^+\right)^2 e^{2ik_1 z} + \left(A_1^-\right)^2 e^{-2ik_1 z} + 2A_1^+A_1^-\right) \end{aligned} \ . \tag{A4}$$

With the slowly-varying amplitude approximation

$$\left|\frac{d^2A_2^+}{dz^2}\right| \ll \left|k_2\frac{dA_2^+}{dz}\right|, \left|\frac{d^2A_2^-}{dz^2}\right| \ll \left|-k_2\frac{dA_2^-}{dz}\right| \tag{A5}$$

and taking into account that $k_2^2 = \varepsilon_2\omega_2^2/c^2$ wave equation Eq.A6 will become

$$ik_2\frac{dA_2^+}{dz}e^{ik_2 z} - ik_2\frac{dA_2^-}{dz}e^{-ik_2 z} = C\left(\left(A_1^+\right)^2 e^{2ik_1 z} + \left(A_1^-\right)^2 e^{-2ik_1 z} + 2A_1^+A_1^-\right) , \tag{A6}$$

Where $C = 8\pi d_{eff}\omega_2^2/c^2$. Denoting $\Delta k = 2k_1 - k_2$ will give

$$\left(ik_2\frac{dA_2^+}{dz} - C\left(A_1^+\right)^2 e^{i\Delta kz}\right)e^{ik_2 z} - \left(ik_2\frac{dA_2^-}{dz} - C\left(A_1^-\right)^2 e^{-i\Delta kz}\right)e^{-ik_2 z} = 2CA_1^+A_1^- \ . \tag{A7}$$

Right part of the equation does not depend on the z and $e^{ik_2 z}$ and $e^{-ik_2 z}$ functions linearly independent in case of $k_2 \neq 0$, thus, two terms in the left side should be constants (do not depend on z). Let's denote them B_1 and B_2, where $B_1 - B_2 = 2CA_1^+A_1^-$. Then, instead of Eq.A9, there will become a couple of equations

$$\begin{cases} ik_2\dfrac{dA_2^+}{dz} - C\left(A_1^+\right)^2 e^{i\Delta kz} = B_1 e^{-ik_2 z} \\ ik_2\dfrac{dA_2^-}{dz} + C\left(A_1^-\right)^2 e^{-i\Delta kz} = B_2 e^{ik_2 z} \end{cases} . \tag{A8}$$

After integration of this equations in the limits from 0 to l

$$\begin{cases} ik_2\left(A_2^+(l) - A_2^+(0)\right) - C\left(A_1^+\right)^2\dfrac{e^{i\Delta kl} - 1}{i\Delta k} = B_1\dfrac{e^{-ik_2 l} - 1}{-ik_2} \\ ik_2\left(A_2^-(l) - A_2^-(0)\right) + C\left(A_1^-\right)^2\dfrac{e^{-i\Delta kl} - 1}{-i\Delta k} = B_2\dfrac{e^{ik_2 l} - 1}{ik_2} \end{cases} . \tag{A9}$$

After some simplifications

$$\begin{cases} ik_2\left(A_2^+(l)-A_2^+(0)\right)-Cl\left(A_1^+\right)^2 e^{i\frac{\Delta kl}{2}}\,\mathrm{sinc}\left(\frac{\Delta kl}{2}\right)=B_1 l e^{-i\frac{k_2 l}{2}}\,\mathrm{sinc}\left(\frac{k_2 l}{2}\right) \\ ik_2\left(A_2^-(l)-A_2^-(0)\right)+Cl\left(A_1^-\right)^2 e^{-i\frac{\Delta kl}{2}}\,\mathrm{sinc}\left(\frac{\Delta kl}{2}\right)=B_2 l e^{i\frac{k_2 l}{2}}\,\mathrm{sinc}\left(\frac{k_2 l}{2}\right) \end{cases}. \quad \text{(A10)}$$

Note that right sights of the Eq.A12 are negligible due to the $\mathrm{sinc}(k_2 l/2)=\sin(k_2 l/2)/(k_2 l/2)$ term, and hereafter, right parts will be omitted.

Solution of the equation should satisfy following boundary conditions

$$\begin{cases} A_2^-(l)=r_2' A_2^+(l)e^{2ik_2 l} \\ A_2^+(0)=r_1' A_2^-(0) \end{cases}, \quad \text{(A11)}$$

which are actually reflection laws at the boundaries of the nonlinear crystal. r_1' and r_2' are amplitude reflection coefficients of the first and second edges for SH wave.

Solution of the equations for the forward propagating wave near the output edge in the crystal ($A_2^+(l)$) is given by the following formula

$$A_2^+(l)=Cl\,\mathrm{sinc}\left(\frac{\Delta kl}{2}\right)\frac{\left(A_1^+\right)^2 e^{i\frac{\Delta kl}{2}}+r_1'\left(A_1^-\right)^2 e^{-i\frac{\Delta kl}{2}}}{ik_2(1-r_1' r_2' e^{2ik_2 l})}. \quad \text{(A12)}$$

Intensity of the SH output power is proportional to the square of the absolute value of the $A_2^+(l)$ multiplied with the transmission coefficient of the output surface.

$$I_2 \propto \left|t_2' A_2^+(l)\right|^2. \quad \text{(A13)}$$

In case of quasi-phase matched SHG Δk is equal to

$$\Delta k = 2k_1 - k_2 - \frac{1}{\Lambda}, \quad \text{(A14)}$$

where Λ is the period of domain structure in the periodic polled nonlinear crystal.

References

[1] W. P. Risk, T. R. Gosnell and A. V. Nurmikko, Compact blue-green lasers, Cambridge University Press, Cambridge (2003)

[2] N. Bloembergen and P. S. Pershan, Phys. Rev. 128(2) (1962) 606 – 622

[3] J. P. Van Der Ziel, IEEE J. Quantum Electron., QE-12(7) (1976) 407 – 411

[4] R. Morita, T. Kondo, Y. Kaneda, A. Sugihashi, N. Ogasawara and S. Umegaki, Jap. J. Appl. Phys. 27(6) (1988) L1134 – L1136

[5] Y. Hase, K. Kumata, S. S. Kano, M. Ohashi, T. Kondo, R. Ito and Y, Shiraki, Appl. Phys. Lett. 61(145) (1992) 145 – 146

[6] W. N. Herman and L. M. Hayden, J. Opt. Soc. Am. B 13(3) (1995) 416 – 427

[7] H. Hellwig and L. Bohatý, Opt. Comm. 161 (1999) 51 – 56

[8] G. Telier, C. Boisrobert, Opt. Comm. 279 (2007) 183 – 195

[9] S. Essaian, J. Khaydarov, S. Slavov, V. Ter-Mikirtychev, G. Gabrielyan, M. Kerobyan, S. Soghomonyan, Proc. of SPIE, 8240 (2012) 82400I-1 – 82400I-8

[10] J. Watanabe and T. Harimoto, Optics Express 15(3) (2007) 965 – 970

[11] Y. Ma, L. Wu, H. Wu, W. Chen, Y. Wang, and S. Gu, Optics Express 16(23) (2008) 18702 – 18713

[12] J.Z. Sotor, G. Dudzik, A.J. Antonczak and K.M. Abramski, Appl. Phys. B 103 (2011) 67 – 74

[13] S.I. Derzhavin, D.A. Mashkovskii and V.N. Timoshkin, Quantum Electronics 38(12) (2008) 1117 – 1120

[14] M. Kerobyan, A. Gyulasaryan, A. Khachikyan, S. Soghomonyan, G. Gabrielyan and S. Essaian, Opt. Comm. 311 (2013) 38 – 43

[15] M. Kerobyan, Nanosystems: Physics, Chemistry, Mathematics, 2013, 4 (6), P. 772–777

[16] R. Boyd, Nonlinear optics, 3rd ed., Academic Press, New York, (2008)